CHAPTER 15
BIOCERAMICS

David H. Kohn
University of Michigan,
Ann Arbor, Michigan

15.1 INTRODUCTION

The clinical goal when using ceramic biomaterials, as is the case with any biomaterial, is to replace lost tissue or organ structure and/or function. The rationale for using ceramics in medicine and dentistry was initially based upon the relative biological inertness of ceramic materials compared to metals. However, in the past 25 years, this emphasis has shifted more toward the use of bioactive ceramics, materials that elicit normal tissue formation and also form an intimate bond with bone tissue through partial dissolution of the material surface. In the last decade, bioceramics have also been utilized in conjunction with more biological therapies. In other words, the ceramic, usually resorbable, facilitates the delivery and function of a biological agent (i.e., cells, proteins, and/or genes), with an end-goal of eventually regenerating a full volume of functional tissue.

Ceramic biomaterials are processed to yield one of four types of surfaces and associated mechanisms of tissue attachment (Kohn and Ducheyne, 1992): (1) fully dense, relatively inert crystalline ceramics that attach to tissue by either a press fit, tissue growth onto a roughened surface, or via a grouting agent; (2) porous, relatively inert ceramics, where tissue grows into the pores, creating a mechanical attachment between the implant and tissue; (3) fully dense, surface reactive ceramics, which attach to tissue via a chemical bond; and (4) resorbable ceramics that integrate with tissue and eventually are replaced by new or existing host tissue. Ceramics may therefore be classified by their macroscopic surface characteristics (smooth, fully dense, roughened, or porous) or their chemical stability (inert, surface reactive, or bulk reactive/resorbable). The integration of biological (i.e., inductive) agents with ceramics further expands the clinical potential of these materials.

Relatively inert ceramics elicit minimal tissue response and lead to a thin layer of fibrous tissue adjacent to the ceramic surface. Surface-active ceramics are partially soluble, resulting in ion exchange and the potential to lead a direct chemical bond with tissue. Bulk bioactive ceramics are fully resorbable, have greater solubility than surface-active ceramics, and may ultimately be replaced by an equivalent volume of regenerated tissue. The relative level of bioactivity mediates the thickness of the interfacial zone between the biomaterial surface and host tissue (Fig. 15.1).

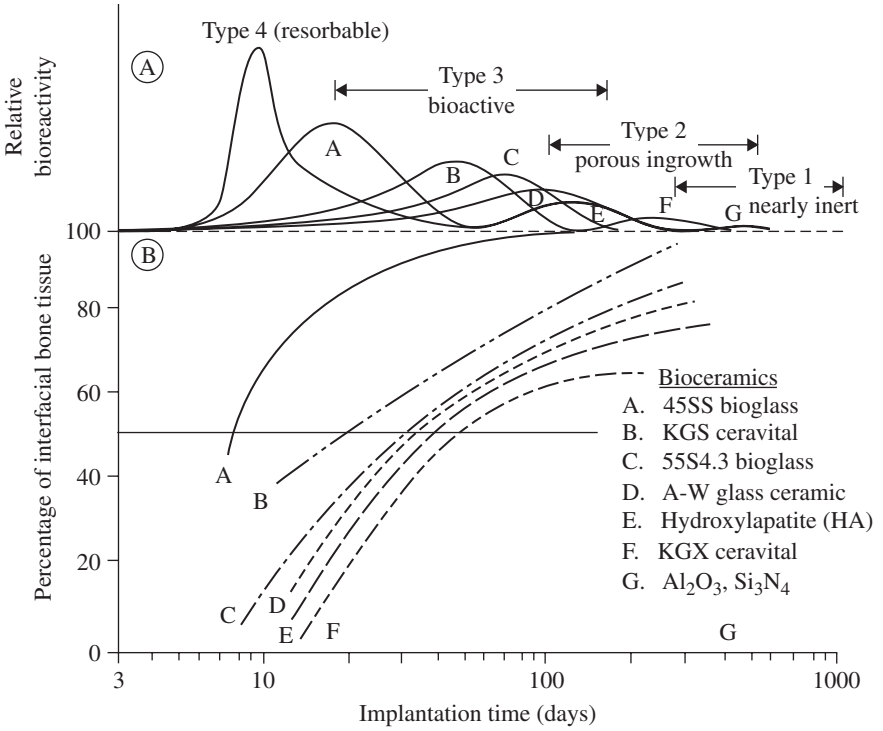

FIGURE 15.1 Bioactivity spectra for selected bioceramics: (*a*) relative magnitudes and rates of bioactivity, (*b*) time dependence of bone formation at bioceramic surface and ceramic/bone bonding. [*From Hench and Best (2004), with permission.*]

There are, however, no standardized measures of "reactivity," but the most common are pH changes, ion solubility, tissue reaction, and any number of assays that assess some parameter of cell function.

Five main ceramic materials are used for musculoskeletal reconstruction and regeneration: carbon (Christel et al., 1987; Haubold et al., 1981; Huttner and Huttinger, 1984), alumina (Al_2O_3) (Kohn and Ducheyne, 1992; Hulbert et al., 1970; Boutin et al., 1988; Heimke et al., 1978; Webster et al., 2000; Zreiqat et al., 1999; Tohma et al., 2006; Nizard et al., 2008), zirconia (ZrO_2) (Kohn and Ducheyne, 1992; Cales and Stefani, 1995; Christel et al., 1989; Filiaggi, et al., 1996), bioactive glasses and glass ceramics (Kohn and Ducheyne, 1992; Ducheyne, 1985; El-Ghannam et al., 1997; Radin et al., 2005; Reilly et al., 2007; Gross and Strunz, 1980; Hench et al., 1972; Nakamura et al., 1985) and calcium phosphates (Kohn and Ducheyne, 1992; Murphy et al., 2000a; Shin et al., 2007; Ducheyne 1987; Ducheyne et al., 1980; Koeneman et al., 1990; Van Raemdonck et al., 1984). Carbon, alumina, and zirconia are considered "bioinert," whereas glasses and calcium phosphates are bioactive.

In this chapter, three types of bioceramics (bioinert, surface bioactive, bulk bioactive) are discussed, with a focus on musculoskeletal applications. A material science approach is taken to address design issues of importance to a biomedical engineer; the processing-structure-composition-property synergy is discussed for each material, then properties important to the design and clinical success of each class of bioceramic are presented. Within the framework of discussing the processing-composition-structure synergy, issues of material selection, service conditions, fabrication routes and characterization methodologies are discussed.

15.2 BIOINERT CERAMICS

Ceramics are fully oxidized materials and are therefore chemically stable and less likely to elicit an adverse biological response than metals, which only oxidize at their surface. Three types of "inert" ceramics are of interest in musculoskeletal applications: carbon, alumina, and zirconia.

15.2.1 Carbon

The benign biological reaction to carbon-based materials, along with the similarity in stiffness and strength between carbon and bone, made carbon a candidate material for musculoskeletal reconstruction almost 40 years ago (Bokros et al., 1972). Carbon has a hexagonal crystal structure that is formed by strong covalent bonds. Graphite has a planar hexagonal array structure, with a crystal size of approximately 1000 Å (Bokros, 1978). The carbon-carbon bond energy within the planes is large (114 kcal/mol), whereas the bond between the planes is weak (4 kcal/mol) (Hench and Ethridge, 1982). Therefore, carbon derives its strength from the strong in-plane bonds, whereas the weak bonding between the planes results in a low modulus, near that of bone (Bokros, 1978).

Isotropic carbon, on the other hand, has no preferred crystal orientation and therefore possesses isotropic material properties. There are three types of isotropic carbon: pyrolytic, vitreous, and vapor deposited. Pyrolytic carbons are formed by the deposition of carbon from a fluidized bed onto a substrate. The fluidized bed is formed from pyrolysis of hydrocarbon gas between 1000 to 2500°C (Hench and Ethridge, 1982). Low temperature isotropic (LTI) carbons are formed at temperatures below 1500°C. LTI pyrolytic carbon possesses good frictional and wear properties, and incorporation of silicon can further increase hardness and wear resistance (Bokros, 1978). Vitreous carbon is a fine-grained polycrystalline material formed by slow heating of a polymer. Upon heating, the more volatile components diffuse from the structure and only carbon remains (Hench and Ethridge, 1982). Since the process is diffusion mediated and potentially volatile, heating must be slow and dimensions of the structure are limited to approximately 7 mm (Bokros, 1978). Salient properties of all three forms of carbon are summarized in Table 15.1.

Deposition of LTI coatings onto metal substrates is limited by the brittleness of the coatings and propensity for coating fracture and coating/substrate debonding (Hench and Ethridge, 1982). Carbon may also be vapor deposited onto a substrate by the evaporation of carbon atoms from a high-temperature source and subsequent condensation onto a low temperature substrate (Hench and Ethridge, 1982). Vapor-deposited coatings are approximately 1 μm thick, allowing properties of the substrate to be retained. More recently, diamondlike carbon (DLC) coatings have been studied, as a means of improving fixation to bone (Koistinen et al., 2005, Reikeras et al., 2004) and wear resistance (Allen et al., 2001). Carbon-based thin films are produced from solid carbon or liquid/gaseous hydrocarbon sources, using ion beam or plasma deposition techniques, and have properties intermediate to those of graphite and diamond (Allen et al., 2001).

With the advent of nanotechnology, interest in carbon has been rekindled, in the form of carbon nanotubes (CNTs). CNTs have been proposed as scaffolds to support osteoconductivity (Zanello et al., 2006) and as a second phase in polymer scaffolds (Shi et al., 2006).

15.2.2 Alumina

High-density, high-purity, polycrystalline alumina is used for femoral stems, femoral heads, acetabular components, and dental implants (Kohn and Ducheyne, 1992; Boutin et al., 1988; Heimke et al., 1978; Tohma et al., 2006; Nizard et al., 2008). More recently, ion-modified and nanostructured Al_2O_3 have been synthesized, to make these bioceramics stronger and more bioactive (Webster et al., 2000; Zreiqat et al., 1999). In addition to chemical stability and relative biological inertness, other attributes of alumina are hardness and wear resistance. Therefore, a main motivation for using alumina in orthopaedic surgery is to increase tribological properties, and many total hip replacements are now designed as modular devices, that is, an alumina femoral head is press-fit onto the neck of a metal femoral stem.

TABLE 15.1 Physical and Mechanical Properties of Bioceramics

Material	Porosity, %	Density, mg/m^3	Modulus, (GPa)	Compressive strength, MPa	Tensile strength, MPa	Flexural strength, MPa	K_{Ic}, $MPa \cdot m^{1/2}$
Graphite	7	1.8	25	–	–	140	–
(isotropic)	12	1.8	20–24	65–95	24–30	45–55	–
	16–20	1.6–1.85	6–13.4	18–58	8–19	14–27	–
	30	1.55	7.1	–	–	–	–
	–	0.1–0.5	–	2.5–30	–	–	–
Pyrolytic	2.7	2.19	28–41	–	–	–	–
graphite, LTI	–	1.3–2	17–28	900	200	340–520	–
	–	1.7–2.2	17–28	–	–	270–550	–
Glassy (vitreous)	–	1.4–1.6	–	–	–	70–205	–
carbon	–	1.45–1.5	24–28	700	70–200	150–200	–
	–	1.38–1.4	23–29	–	–	190–255	–
	≤50	<1.1	7–32	50–330	13–52	–	–
Bioactive	–	–	–	–	56–83	–	–
ceramics and	–	2.8	–	500	–	100–150	–
glass ceramics	31–76	0.65–1.86	2.2–21.8	–	–	4–35	–
Hydroxyapatite	0.1–3	3.05–3.15	7–13	350–450	38–48	100–120	–
	10	2.7	–	–	–	–	–
	30	–	–	120–170	–	–	–
	40	–	–	60–120	–	15–35	–
	2.8–19.4	2.55–3.07	44–48	310–510	–	60–115	–
	2.5–26.5	–	55–110	≤800	–	50–115	–
Tetracalcium phosphate	Dense	3.1	–	120–200	–	–	–
Tricalcium phosphate	Dense	3.14	–	120	–	–	–
Other calcium phosphates	Dense	2.8–3.1	–	70–170	–	–	–
Al_2O_3	0	3.93–3.95	380–400	4000–5000	350	400–500	5–6
	25	2.8–3.0	150	500	–	70	–
	35	–	–	200	–	55	–
	50–75	–	–	80	–	6–11.4	–
ZrO_2, stabilized	0	4.9–5.6	150–200	1750	–	150–900	4–12
(~3% Y_2O_3)	1.5	5.75	210–240	–	–	280–450	–
	5	–	150–200	–	–	50–500	–
	28	3.9–4.1	–	< 400	–	50–65	–

Source: Modified from Kohn and Ducheyne (1992), with permission.

High-purity alumina powder is typically isostatically compacted and shaped. Subsequent sintering at 1600 to 1800°C transforms a preform into a dense polycrystalline solid having a grain size of less than 5 μm (Boutin et al., 1988). Addition of trace amounts of MgO aids in sintering and limits grain growth. If processing is kept below 2050°C, α-Al_2O_3, which is the most stable phase, forms. Alternatively, single crystals (sapphire) may be grown by feeding powder onto a seed and allowing buildup.

The physical and mechanical properties (e.g., ultimate strength, fatigue strength, fracture toughness, wear resistance) of α-alumina are a function of purity, grain size, grain size distribution, porosity, and inclusions (Kohn and Ducheyne, 1992; Boutin et al., 1988; Dorre and Dawihl, 1980) (Table 15.1). The elastic modulus of dense alumina is two-to-four fold greater than that of metals used in bone and joint reconstruction. Both grain size (d) and porosity (P, $0 \le P \le 1$) affect strength (σ) via power law and exponential relations, respectively [Eqs. (15.1) and (15.2)], where σ_0 is the strength of the dense ceramic, A, n, and B are material constants, experimentally determined, and n is approximately 0.5.

$$\sigma = Ad^{-n} \tag{15.1}$$

$$\sigma_P = \sigma_0 e^{-BP} \tag{15.2}$$

For example, decreasing the grain size of Al_2O_3 from 4 to 7 μm increases strength by approximately 20 percent (Dorre and Dawihl, 1980). With advances in ceramic processing, it is now possible to fabricate alumina with grain sizes approximately 1 μm and small grain size distributions, material characteristics that increase strength.

The amount of wear in alumina-alumina bearing couples can be as much as 10 times less than in metal-polyethylene systems (Davidson, 1993; Kumar et al., 1991; Lusty et al., 2007). The coefficients of friction of alumina-alumina and alumina-polyethylene are less than that of metal-polyethylene, because of alumina's low surface roughness and wettability (Boutin et al., 1988; Semlitsch et al., 1977).

The major limitations of alumina are its low tensile and bending strengths and fracture toughness. As a consequence, alumina is sensitive to stress concentrations and overloading. Clinically retrieved alumina total hip replacements exhibit damage caused by fatigue, impact, or overload (Walter and Lang, 1986). Many ceramic failures can be attributed to materials processing or design deficiencies, and can be minimized through better materials choice and quality control.

15.2.3 Zirconia

Yttrium oxide partially stabilized zirconia (YPSZ) is an alternative to alumina, and there are approximately 150,000 zirconia components in clinical use (Christel et al., 1989; Cales and Stefani, 1995). YPSZ has a higher toughness than alumina, since it can be transformation toughened, and is used in bulk form or as a coating (Filiaggi et al., 1996).

At room temperature, pure zirconia has a monoclinic crystal symmetry. Upon heating, it transforms to a tetragonal phase at approximately 1000 to 1100°C, and then to a cubic phase at approximately 2000°C (Fig. 15.2). A partially reversible volumetric shrinkage (density increase) of 3 to 10 percent occurs during the monoclinic to tetragonal transformation (Christel et al., 1989). The volumetric changes resulting from the phase transformations can lead to residual stresses and cracking. Furthermore, because of the large volume reduction, pure zirconia cannot be sintered. However, sintering and phase transformations can be controlled via the addition of stabilizing oxides. Yttrium oxide (Y_2O_3) serves as a stabilizer for the tetragonal phase such that upon cooling, the tetragonal crystals are maintained in a metastable state and do not transform back to a monoclinic structure. The tetragonal to monoclinic transformation and volume change are also prevented by neighboring grains inducing compressive stresses on one another (Christel et al., 1989).

The modulus of partially stabilized zirconia is approximately half that of alumina, while the bending strength and fracture toughness are 2 to 3 and 2 times greater, respectively (Table 15.1). The relatively high strength and toughness are a result of transformation toughening, a mechanism that manifests itself as follows (Fig. 15.3): crack nucleation and propagation lead to locally elevated stresses and energy in the tetragonal crystals surrounding the crack tip. The elevated energy induces the metastable tetragonal grains to transform into monoclinic grains in this part of the microstructure. Since the monoclinic grains are larger than the tetragonal grains, there is a local volume increase, compressive stresses are induced, more energy is needed to advance the crack, and crack blunting occurs.

The wear rate of YPSZ on UHMWPE can be 5 times less than the wear rate of alumina on UHMWPE, depending on experimental conditions (Kumar et al., 1991; Davidson, 1993; Derbyshire et al., 1994). Wear resistance is a function of grain size, surface roughness, and residual compressive stresses induced by the phase transformation. The increased mechanical and tribological properties of zirconia may allow for smaller diameter femoral heads to be used in comparison to alumina.

Partially stabilized zirconia is typically shaped by cold isostatic pressing and then densified by sintering. Sintering may be performed with or without a subsequent hot isostatic pressing (HIP-ing) cycle. The material is usually presintered until approximately 95 percent dense and then HIP-ed to remove residual porosity (Christel et al., 1989). Sintering can be performed without inducing grain growth, and final grain sizes can be less than 1 μm.

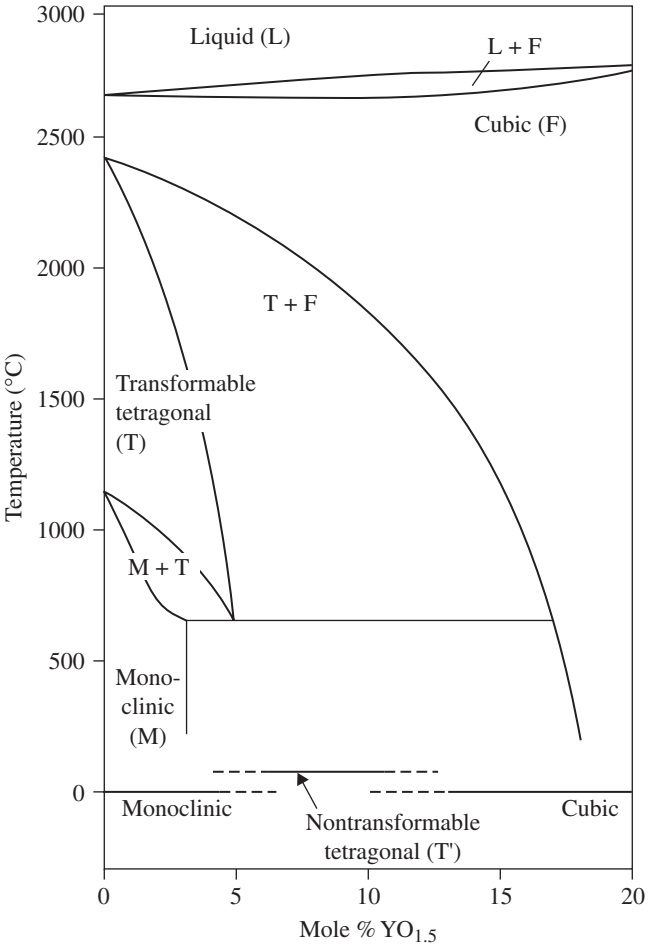

FIGURE 15.2 Schematic phase diagram of the ZrO_2–Y_2O_3 system. [*From Cales and Stefani (1995), with permission.*]

15.2.4 Critical Properties of Bioinert Ceramics

Properties of bioinert ceramics important for their long-term clinical function include stiffness, strength, toughness, wear resistance, and biological response. Stiffness represents one gauge of the mechanical interaction between an implant and its surrounding tissue, it is one determinant of the magnitude and distribution of stresses in a biomaterial and tissue, and dictates, in part, the potential for stress shielding (Kohn and Ducheyne, 1992; Ko et al., 1995). Load-bearing biomaterials must also be designed to ensure that they maintain their structural integrity, that is, designed to be fail-safe at stresses above peak in-service stresses for a lifetime greater than the expected service life of the prosthesis. Thus, the static (tensile, compressive, and flexural strength), dynamic (high-cycle fatigue) and toughness properties of ceramics, in physiological media, under a multitude of loading conditions and rates must be well-characterized.

Although knowledge of these properties is an important aspect of bioceramic design, the mechanical integrity of a bioceramic is also dependent on its processing, size, and shape. Failure of ceramics

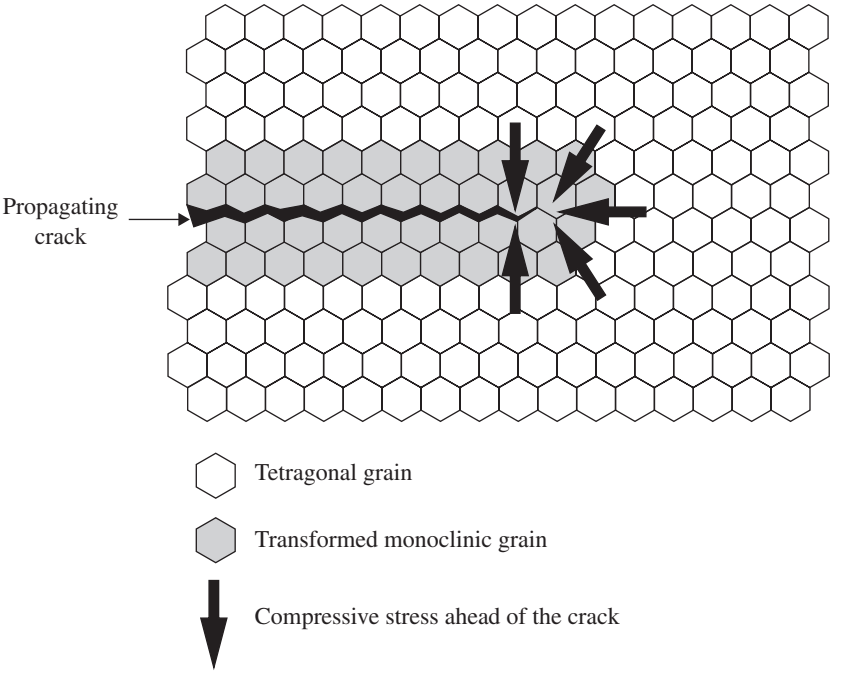

FIGURE 15.3 Schematic of microstructure in yttria partially stabilized zirconia (YPSZ) bioceramic undergoing transformation toughening at a crack tip. (*From Miller et al. (1981), with permission.*]

usually initiates at a critical defect, at a stress level that depends on the geometry of the defect. To account for these variables and minimize the probability of failure, fracture mechanics and statistical distributions are used to predict failure probability at different load levels (Soltesz and Richter, 1984).

15.3 BIOACTIVE CERAMICS

The concept of bioactivity originated with bioactive glasses via the hypothesis that the biocompatibility of an implant is optimal if it elicits the formation of normal tissues at its surface, and if it establishes a contiguous interface capable of supporting the loads which occur at the site of implantation (Hench et al., 1972). Under appropriate conditions, three classes of ceramics may fulfill these requirements: bioactive glasses and glass ceramics, calcium phosphate ceramics, and composites of glasses and ceramics. Incorporation of inductive factors into each of these ceramics may enhance bioactivity. These different classes of ceramics (and biological constituents) are used in a variety of applications, including: bulk implants (surface active), coatings on metal or ceramic implants (surface active), permanent bone augmentation devices/scaffold materials (surface active), temporary scaffolds for tissue engineering (surface or bulk active), fillers in cements or scaffolds (surface or bulk active), and drug delivery vehicles (bulk active).

The nature of the biomaterial/tissue interface and reactions (e.g., ion exchange) at the ceramic surface and adjacent tissues dictate the resultant mechanical, chemical, physical, and biological properties. Four factors determine the long-term effect of bioactive ceramic implants: (1) the site of implantation, (2) tissue trauma, (3) the bulk and surface properties of the material, and (4) the relative

motion at the implant/tissue interface (Ducheyne et al., 1987). For resorbable materials, additional design requirements include: the need to maintain strength and stability of the material/tissue interface during material degradation and host tissue regeneration; material resorption and tissue repair/regeneration rates should be matched; and the resorbable material should consist only of metabolically acceptable species.

15.3.1 Bioactive Glasses and Glass Ceramics

Bioactive glasses are used as bulk implants, coatings on metal or ceramic implants, and scaffolds for guiding biological therapies (Kohn and Ducheyne, 1992; Hench et al., 1972; El-Ghannam et al., 1997; Gross and Strunz, 1980; Nakamura et al., 1985; Radin et al., 2005; Reilly et al., 2007) (Table 15.2). Chemical reactions are limited to the surface (~300 to 500 μm) of the glass, and bulk properties are not affected by surface reactivity. The degree of activity and physiologic response are dependent on the chemical composition of the glass, and may vary by over an order of magnitude. For example, the substitution of CaF for CaO decreases solubility, while addition of B_2O_3 increases solubility (Hench and Ethridge, 1982).

Ceravital, a variation of ~~Bioglass~~, is a glass ceramic. The seed material is quench-melted to form a glass, then heat-treated to form nuclei for crystal growth and transformation from a glass to a ceramic. Ceravital has a different alkali oxide concentration than ~~bioglass~~—small amounts of alkaline oxides are added to control dissolution rates (Table 15.2)—but the physiological response to both glasses is similar (Gross and Strunz, 1980). A glass ceramic containing crystalline oxyapatite, fluorapatite, and β-Wollastonite in a glassy matrix, denoted glass-ceramic A-W, is another bioactive glass ceramic (Kitsugi et al., 1986; Kokubo et al., 1990a, 1990b; Nakamura et al., 1985). A-W glass-ceramic bonds to bone through a thin calcium and phosphorus-rich layer, which is formed at the surface of the glass ceramic (Kitsugi et al., 1986; Nakamura et al., 1985). In vitro, if the physiological environment is correctly simulated in terms of ion concentration, pH, and temperature, this layer consists of small carbonated hydroxyapatite (HA) crystallites with a defective structure, and the composition and structural characteristics are similar to those of bone (Kokubo et al., 1990a).

Glass and glass-ceramics interface with the biological milieu because ceramics are susceptible to surface changes in an aqueous media. Lower valence ions segregate to surfaces and grain boundaries, leading to concentration gradients and ion exchange. These reactions are dependent on the local pH and reactive cellular constituents (Hench and Ethridge, 1982), and can be biologically beneficial or adverse. Therefore, the surface reactions of glass ceramics should be well-controlled and characterized.

When placed in physiological media, bioactive glasses leach Na^+ ions, and subsequently K^+, Ca^{2+}, P^{5+}, Si^{4+}, and Si-OH. These ionic species are replaced with H_3O^+ ions from the media through

TABLE 15.2 Composition (Weight Percent) of Bioactive Glasses and Glass Ceramics

Material	45S5 Bioglass	45S5-F Bioglass	45S5-B5 Bioglass	52S4.6 Bioglass	Ceravital	Stabilized ceravital	A-W Glass ceramic
SiO_2	45.0	45.0	45.0	52.0	40–50	40–50	34.2
P_2O_5	6.0	6.0	6.0	6.0	10–15	7.5–12.0	16.3
CaO	24.5	12.3	24.5	21.0	30–35	25–30	44.9
Na_2O	24.5	24.5	24.5	21.0	5–10	3.5–7.5	–
B_2O_3	–	–	5.0	–	–	–	–
CaF_2	–	12.3	–		–	–	0.5
K_2O	–	–	–	–	0.5–3.0	0.5–2.0	–
MgO	–	–	–	–	2.5–5.0	1.0–2.5	4.6
Al_2O_3	–	–	–	–	–	5.0–15.0	–
TiO_2	–	–	–	–	–	1.0–5.0	–
Ta_2O_5	–	–	–	–	–	5.0–15.0	–

Source: From Kohn and Ducheyne (1992), with permission.

an ion-exchange reaction which produces a silica-rich gel surface layer (Hench and Ethridge, 1982). In an in vitro setting at least, the depletion of H^+/H_3O^+ ions in solution causes a pH increase, which further drives dissolution of the glass surface. With increasing time of exposure to media, the high-surface-area silica-rich surface gel chelates calcium and phosphate ions, and a Ca-P-rich, amorphous apatite layer forms on top of the silica-rich layer. This Ca-P-rich layer may form after as little as 1 hour in physiological solution (Hench and Ethridge, 1982). The amorphous Ca-P layer eventually crystallizes and CO_3^{2-} substitutes for OH^- in the apatite lattice, leading to the formation of a carbonated apatite layer. Depending on animal species, anatomic, site and time of implantation, the steady-state thickness of the Ca-P-rich and Si-rich zones can range from 30 to 70 μm and 60 to 230 μm, respectively (Hench and Ethridge, 1982).

In parallel with these physical/chemical-mediated reactions, in an in vivo setting, proteins adsorb/desorb from the silica gel and carbonate layers. The bioactive surface and preferential protein adsorption that can occur on the surface can enhance attachment, differentiation, and proliferation of osteoblasts and secretion of an extracellular matrix (ECM). Crystallization of carbonated apatite within an ordered collagen matrix leads to an interfacial bond.

The overall rate of change of the glass surface R is quantified as the sum of the reaction rates of each stage of the reaction (Hench and Best, 2004):

$$R = -k_1 t^{0.5} - k_2 t^{1.0} + k_3 t^{1.0} + k_4 t^{y} + k_5 t^{z} \tag{15.3}$$

where k_i is the rate constant for each stage, i and represents, respectively, the rate of exchange between alkali cations in glass and H^+/H_3O^+ in solution (k_1), interfacial SiO_2 network dissolution (k_2), repolymerization of SiO_2 (k_3), carbonate precipitation and growth (k_4), and other precipitation reactions (k_5). Using these ~~rates~~, the following design criterion may be established: the kinetics of each stage, especially stage 4, should match the rate of biomineralization in vivo. For $R >>$ in vivo rates, resorption will occur, whereas if $R <<$ in vivo rates, the glass will be nonbioactive (Hench and Best, 2004).

The degree of activity and physiological response (e.g., rates of formation of the Ca-P surface and glass/tissue bond) therefore ~~depends~~ on the glass composition and time, and is mediated by the biomaterial, solution, and cells. The dependence of reactivity and rate of bond formation on glass composition is defined by the ratio of network former to network modifier: $SiO_2/[CaO + Na_2O + K_2O]$ (Hench and Clark, 1982). The higher this ratio is, the less soluble is the glass, and the slower is the rate of bone formation. A SiO_2-Na_2O-CaO ternary diagram (Fig. 15.4) is useful to quantify the relationship between composition and biological response (Hench and Best, 2004). The diagram may be divided into three zones: zone A—bioactive bone bonding: glasses are characterized by CaO/P_2O_5 ratios > 5 and $SiO_2/[CaO + Na_2O] < 2$; zone B—nearly inert: bone bonding does not occur (only fibrous tissue formation occurs), because the SiO_2 content is too high and reactivity is too low—these high SiO_2 glasses develop only a surface hydration layer or too dense of a silica-rich layer to enable further dissolution and ion exchange; zone C—resorbable glasses: no bone bonding occurs because reactivity is too high and SiO_2 undergoes rapid selective alkali ion exchange with protons or H_3O^+, leading to a thick but porous unprotected SiO_2-rich film that dissociates at a high rate.

The level of bioactivity is related to bone formation via an index of bioactivity I_B, which is related to the amount of time it takes for 50 percent of the interface to be bonded (Hench and Best, 2004):

$$I_B = 100/t_{0.5BB} \tag{15.4}$$

The compositional dependence of the biological response may be understood by iso-I_B contours superposed onto the ternary diagram (Fig. 15.4). The cohesion strength of the glass/tissue interface will be a function of surface area, thickness, and stiffness of the interfacial zone, and is optimum for $I_B \sim 4$ (Hench and Best, 2004).

15.3.2 Calcium-Phosphate Ceramics

Calcium-phosphate (Ca-P) ceramics are ceramics with varying calcium-to-phosphate ratios. Among the Ca-Ps, the apatites, defined by the chemical formula $M_{10}(XO_4)_6Z_2$, have been studied most and are most relevant to ~~biomaterials Apatites~~ form a range of solid solutions as a result of ion substitution

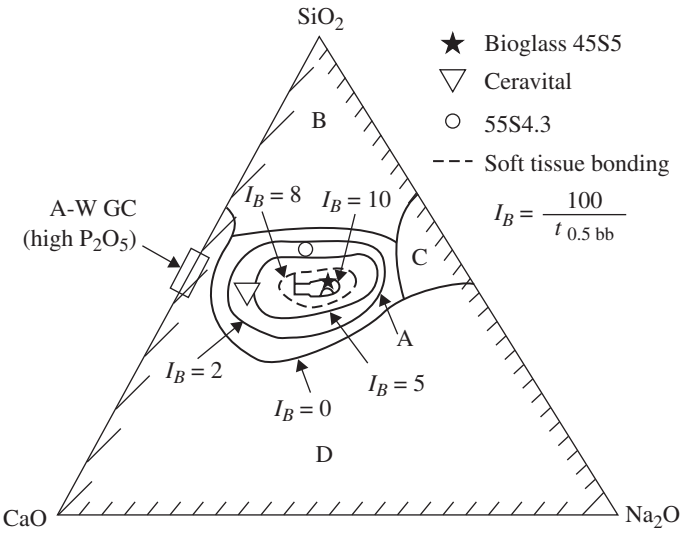

FIGURE 15.4 Ternary diagram (SiO_2-Na_2O-CaO, at fixed 6 percent P_2O_5) showing the compositional dependence (in weight percent) of bone bonding and fibrous tissue bonding to the surfaces of bioactive glasses and glass ceramics: zone A: bioactive bone bonding ceramics; zone B: nearly inert ceramics—bone bonding does not occur at the ceramic surface, only fibrous tissue formation occurs; zone C: resorbable ceramics—no bone bonding occurs because reactivity is too high; I_B = index of bioactivity for bioceramics in zone A. [*From Hench and Best (2004), with permission*.]

at the M^{2+}, XO_4^{3-}, or Z^- sites. Apatites are usually nonstoichiometric and contain less than 10 mol of M^{2+} ions, less than 2 mol of Z^- ions, and exactly 6 mol of XO_4^{3-} ions (Van Raemdonck et al., 1984). The M^{2+} species is typically a bivalent metallic cation, such as Ca^{2+}, Sr^{2+} or Ba^{2+}, ~~Pb^{2+}~~, ~~or~~ ~~Cd^{2+}~~, the XO_4^{3-} species is typically PO_4^{3-}, VO_4^{3-}, CrO_4^{3-} or MnO_4^{3}, and the monovalent Z^- ions are usually OH^-, F^-, or Br^- (Van Raemdonck et al., 1984).

More complex ionic structures may also exist. For example, replacing the two monovalent Z^- ions with a bivalent ion, such as CO_3^{2-}, results in the preservation of charge neutrality, but one anionic position becomes vacant. Similarly, the M^{2+} positions may also have vacancies. In this case, charge neutrality is maintained by vacancies at the Z^- positions or by substitution of trivalent PO_4^{3-} ions with bivalent ions (Van Raemdonck et al., 1984).

The most common apatite used in medicine and dentistry is hydroxyapatite, a material with the chemical formula $Ca_{10}(PO_4)_6(OH)_2$, denoting that 2 formula units are represented within each unit cell (Fig. 15.5). HA has ideal weight percents of 39.9 percent Ca, 18.5 percent P, and 3.38 percent OH, and an ideal Ca/P ratio of 1.67. The crystal structure and crystallization behavior of HA are affected by ionic substitutions.

The impetus for using synthetic HA as a biomaterial stems from the hypothesis that a material similar to the mineral phase in bone and teeth will have superior binding to mineralized tissues and is, therefore, advantageous for replacing these tissues. Additional advantages of bioactive ceramics include low thermal and electrical conductivity, elastic properties similar to those of bone, control of in vivo degradation rates through control of material properties, and the potential for ceramic to function as a barrier when coated onto a metal substrate (Koeneman et al., 1990).

The HA in bone is nonstoichiometric, has a Ca/P ratio less than 1.67, and also contains carbonate, sodium, magnesium, fluorine, and chlorine (Posner, 1985a). Most synthetic hydroxyapatites contain substitutions for the PO_4^{3-} and/or OH^- groups and therefore vary from the ideal stoichiometry and Ca/P ratios. Oxyhydroxyapatite, tricalcium phosphate, tetracalcium phosphate, and ~~octocalcium~~ phosphate have all been detected in commercially available apatite implants (Table 15.3) (Kohn and Ducheyne, 1992; Ducheyne et al., 1986, 1990; Koch et al., 1990).

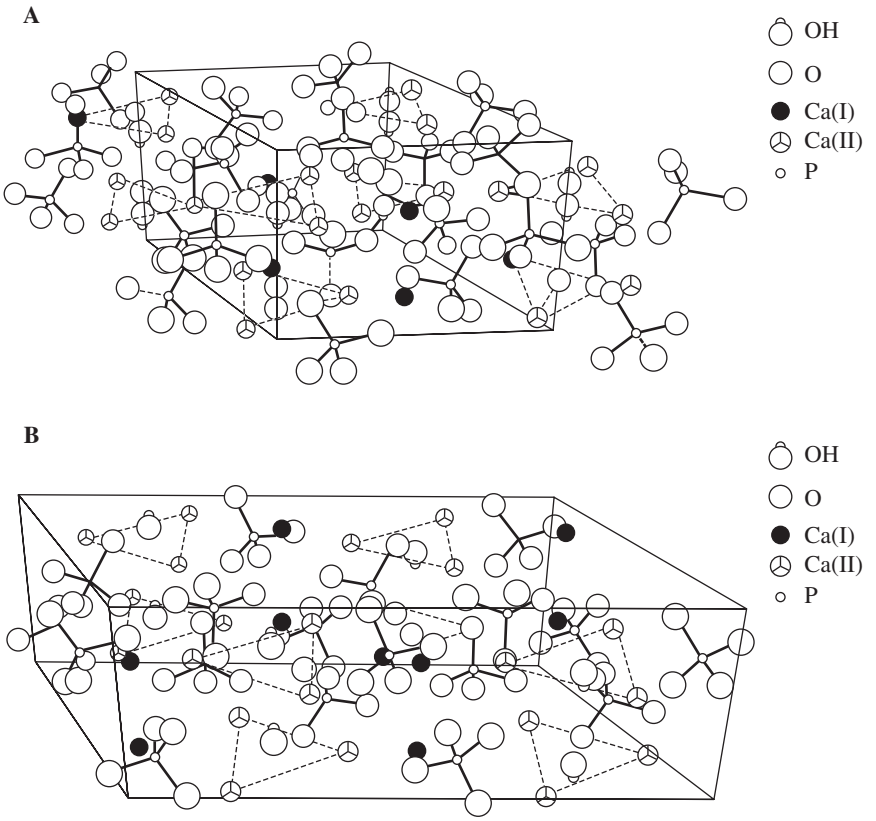

FIGURE 15.5 Schematic of hydroxyapatite crystal structure: (*a*) hexagonal, (*b*) monoclinic. [*From Kohn and Ducheyne (1992), with permission.*]

TABLE 15.3 Calcium-Phosphate Phases with Corresponding Ca/P Ratios

Name	Formula	Ca/P Ratio
Hydroxyapatite (HA)	$Ca_{10}(PO_4)_6(OH)_2$	1.67
Fluorapatite	$Ca_{10}(PO_4)_6F_2$	1.67
Chlorapatite	$Ca_{10}(PO_4)_6Cl_2$	1.67
A-type carbonated apatite (unhydroxylated)	$Ca_{10}(PO_4)_6CO_3$	1.67
B-type carbonated hydroxyapatite (dahllite)	$Ca_{10-x}[(PO_4)_{6-2x}(CO_3)_{2x}](OH)_2$	≥1.67
Mixed A and B-type carbonated apatites	$Ca_{10-x}[(PO_4)_{6-2x}(CO_3)_{2x}]CO_3$	≥1.67
HPO_4 containing apatite	$Ca_{10-x}[(PO_4)_{6-x}(HPO_4)_x](OH)_{2-x}$	≤1.67
Monohydrate calcium phosphate (MCPH)	$Ca(H_2PO_4)_2H_2O$	0.50
Monocalcium phosphate ~~(MCP)~~	$Ca(H_2PO_4)_2$	0.50
Dicalcium phosphate dihydrate (DCPD)	$Ca(HPO_4)\cdot 2H_2O$	1.00
Tricalcium phosphate (TCP)	α and β-$Ca_3(PO_4)_2$	1.50
Octacalcium phosphate (OCP)	$Ca_8H(PO_4)_6\cdot 5H_2O$	1.33

Source: Adopted from Segvich et al. (2008c), with permission.

Synthetic apatites are processed via hydrolysis, hydrothermal synthesis and exchange, sol-gel techniques, wet chemistry, and conversion of natural bone and coral (Koeneman et al., 1990). Differences in the structure, chemistry, and composition of apatites arise from differences in processing techniques, time, temperature, and atmosphere. Understanding the processing-composition-structure-processing synergy for calcium phosphates is therefore critical to understanding the in vivo function of these materials. For example, as stoichiometric HA is heated from room temperature, it becomes dehydrated. Between 25 and 200°C, adsorbed water is reversibly lost. Between 200 and 400°C, lattice-bound water is irreversibly lost, causing a contraction of the crystal lattice. At temperatures above 850°C, reversible weight loss occurs, indicating another reversible dehydration reaction. Above 1050°C, HA may decompose into β-TCP and tetracalcium phosphate (Van Raemdonck et al., 1984), and at temperatures above 1350°C, β-TCP transforms into α-TCP. Analogous reactions occur with nonstoichiometric HA, but the reaction products differ, as a function of the Ca/P ratio (Van Raemdonck et al., 1984).

The mechanism of biological bonding to calcium phosphates is as follows (de Bruijn et al., 1995). Differentiated osteoblasts secrete a mineralized matrix at the ceramic surface, resulting in a narrow, amorphous electron-dense band approximately 3 to 5 μm thick. Collagen bundles form between this zone and cells. Bone mineral crystals nucleate within this amorphous zone in the form of an ~~octo~~-calcium phosphate precursor phase and, ultimately, undergo a conversion to HA. As the healing site matures, the bonding zone shrinks to about 0.05 to 0.2 μm, and bone attaches through a thin epitaxial layer as the growing bone crystals align with apatite crystals of the material.

Calcium-phosphate-based bioceramics have also been used as coatings on dense implants and porous surface layers to accelerate fixation to tissue (Kohn and Ducheyne, 1992; Cook et al., 1992; Ducheyne et al., 1980; Oonishi et al., 1994). Bond strength to bone, solubility, and in vivo function vary, suggesting a window of material variability in parallel with a window of biological variability.

Processing techniques used to bond Ca-P powders to substrates include plasma and thermal-spraying (de Groot et al., 1987; Koch et al., 1990), sintering (de Groot, 1983; Ducheyne, et al., 1986, 1990), ion-beam, and other sputter techniques (Ong et al., 1991; Wolke et al., 1994), electrophoretic deposition (Ducheyne et al., 1986,1990), sol-gel techniques (Chai et al., 1998), pulsed laser deposition (Garcia et al., 1998), and chemical vapor deposition (Gao et al., 1999).

Different structures and compositions of Ca-P coatings result from different processing approaches, and modulate biological reactions. For example, increased Ca/P ratios, fluorine and carbonate contents, and degree of crystallinity lead to greater stability of the Ca-P (Posner, 1985b, Van Raemdonck et al., 1984). Calcium phosphates with Ca/P ratios in the range 1.5 to 1.67 yield the most beneficial tissue response.

15.3.3 Bioactive Ceramic Composites

Bioactive ceramics typically exhibit low strength and toughness. The design requirement of bioactivity supercedes any mechanical property requirement and, as a result, mechanical properties are restricted. Bioceramic composites have therefore been synthesized as a means of increasing the mechanical properties of bioactive materials. Three approaches are used in developing bioceramic composites: (1) utilize the beneficial biological response to bioceramics, but reinforce the ceramic with a second phase as a strengthening mechanism; (2) utilize bioceramic materials as the second phase to achieve desirable strength and stiffness; and (3) synthesize transient scaffold materials for tissue (re)generation (Ducheyne, 1987).

Bioactive glass composites have been synthesized via thermal treatments that create a second phase (Gross and Strunz, 1980, 1985; Kitsugi et al., 1986). By altering the firing temperature and composition of the bioactive glass, stable multiphase bioactive glass composites have been produced. Adding oxyapatite, fluorapatite, β-Wollastonite, and/or β-Whitlockite results in bending strengths 2 to 5 times greater than that of unreinforced bioactive glasses (Kitsugi et al., 1986). Calcium phosphates have been strengthened via incorporation of glasses, alumina, and zirconia (Ioku et al., 1990; Knowles and Bonfield, 1993; Li et al., 1995).

15.3.4 Critical Properties of Bioactive Ceramics

Important needs in bioactive ceramics research and development include characterization of the processing-composition-structure-property synergy, characterization of in vivo function, and establishing predictive relationships between in vitro and in vivo outcomes. Understanding reactions at the ceramic surface and improving the ceramic/tissue bond depend on (Ducheyne, 1987) (1) characterization of surface activity, including surface analysis, biochemistry, and ion transport; (2) physical chemistry, pertaining to strength and degradation, stability of the tissue/ceramic interface and tissue resorption; and (3) biomechanics, as related to strength, stiffness, design, wear, and tissue remodeling. These properties are time dependent and should be characterized as functions of loading and environmental history.

Physical/chemical properties that are important to characterize and relate to biological response include powder particle size and shape, pore size, shape and distribution, specific surface area, phases present, crystal structure and size, grain size, density, coating thickness, hardness, and surface roughness.

Starting powders may be identified for their particle size, shape, and distribution, via sifting techniques or quantitative stereology. Pore size, shape, and distribution, important properties with respect to strength and bioreactivity, may be quantified via stereology and/or SEM. Specific surface area, important in understanding the dissolution and precipitation reactions at the ceramic/fluid interface, may be characterized by B.E.T. Phase identification may be accomplished via XRD and FTIR. Grain sizes may be determined through optical microscopy, SEM, or TEM. Auger electron spectroscopy (AES) and x-ray photoelectron spectroscopy (XPS) may also be utilized to determine surface and interfacial compositions. Chemical stability and surface activity may be analyzed via XPS and measurements of ionic fluxes and zeta potentials.

An additional factor that should be considered in evaluating chemical stability and surface activity of bioceramics is the aqueous microenvironment and how closely it simulates the in vivo environment. The type and concentration of electrolytes in solution and the presence of proteins or cells may influence how the ceramic surface changes when it interacts with a solution. For example, a solution with constituents, concentrations and pH equivalent to human plasma most accurately reproduces surface changes observed in vivo, whereas more standard buffers do not reproduce these changes (Kokubo et al., 1990b).

The integrity of a biomaterial/tissue interface is dependent on both the implant and tissue. Therefore, both of these constituents should be well characterized: the implant surface should be analyzed and the species released into the environment and tissues should also be determined. Surface analyses can be accomplished with solution chemical methods, such as atomic absorption spectroscopy; physical methods, such as thin film XRD, electron microprobe analysis (EMP), energy dispersive x-ray analysis (EDXA), ~~FTIR,~~ and surface-sensitive methods, such as AES, XPS, and secondary ions mass spectroscopy (SIMS) (Fig. 15.6). The integrity of an implant/tissue interface also depends on the loading pattern, since loading may alter the chemical and mechanical behavior of the interface.

The major factors limiting expanded use of bioactive ceramics are their low-tensile strength and fracture toughness. The use of bioactive ceramics in bulk form is therefore limited to functions in which only compressive loads are applied. Approaches that may allow ceramics to be used in sites subjected to tensile stresses include (1) use of the bioactive ceramic as a coating on a metal or ceramic substrate (Ducheyne et al., 1980), (2) strengthening the ceramic, such as via crystallization of glass (Gross et al., 1981), (3) use fracture mechanics as a design approach (Ritter et al., 1979), and (4) reinforcing the ceramic with a second phase (Ioku et al., 1990; Kitsugi et al., 1986; Knowles and Bonfield, 1993; Li et al., 1995).

No matter which of these strategies is used, the ceramic must be stable, both chemically and mechanically, until it fulfills its intended function(s). The property requirements depend upon the application. For example, if a metallic total hip prosthesis is to be fixed to bone by coating the stem with a Ca-P coating, then the ceramic/metal bond must remain intact throughout the service life of the prosthesis. However, if the coating will be used on a porous coated prosthesis with the intent of accelerating ingrowth into the pores of the metal, then the ceramic/metal bond need only be stable until tissue ingrowth is achieved. In either scenario, mechanical testing of the ceramic/metal bond,

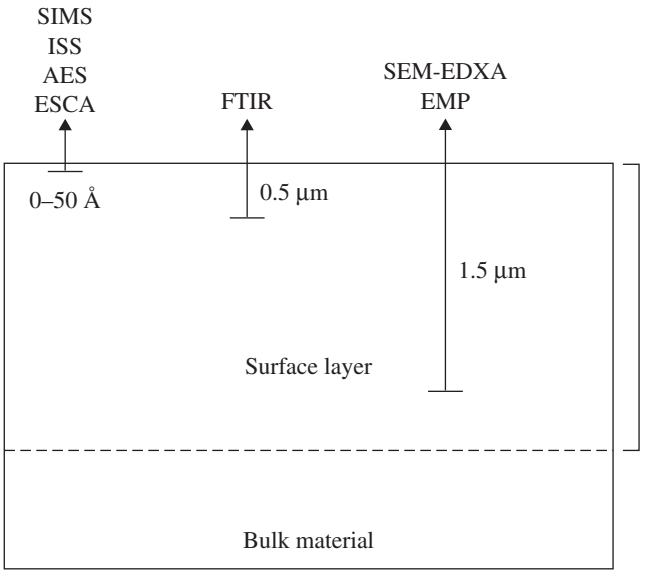

FIGURE 15.6 Schematic of sampling depths for different surface analysis techniques used to characterize bioceramics. [*From Kohn and Ducheyne (1992), with permission*.]

which is the weak link in the system (Kohn and Ducheyne, 1992), is critical (Filiaggi et al., 1991, Mann et al., 1994). A number of interfacial bond tests are available, including pull-out, lap-shear, 3 and 4 point bending, double cantilever beam, double torsion, indentation, scratch tests, and interfacial fracture toughness tests (Koeneman et al., 1990, Filiaggi et al., 1991).

15.4 CERAMICS FOR TISSUE ENGINEERING AND BIOLOGICAL THERAPIES

An ideal tissue substitute would possess the biological advantages of an autograft and supply advantages of an allograft (Laurencin et al., 1996), but alleviate the complications each of these grafts is subject to. Such a construct would also satisfy the following design requirements (Yaszemski et al., 1996): (1) biocompatibility, (2) osteoconductivity—it should provide an appropriate environment for attachment, proliferation, and function of osteoblasts or their progenitors, leading to secretion of a new bone ECM, (3) ability to incorporate osteoinductive factors to direct and enhance new bone growth, (4) allow for ingrowth of vascular tissue to ensure survival of transplanted cells and regenerated tissue, (5) mechanical integrity to support loads at the implant site, (6) degradability, with controlled, predictable, and reproducible rate of degradation into nontoxic species that are easily metabolized or excreted, and (7) be easily processed into irregular three-dimensional shapes. Particularly difficult is the integration of criteria (4) and (5) into one design, since transport is typically maximized by maximizing porosity, while mechanical properties are frequently maximized by minimizing porosity.

One strategy to achieve these design goals is to create a composite graft in which autogenous or allogenic cells (primary cells, cell lines, genetically modified cells, or stem cells) are seeded into a degradable biomaterial (scaffold) that serves as an ECM analogue and supports cell adhesion, proliferation, differentiation, and secretion of a natural ECM. Following cell-seeding, cell/scaffold constructs

may be immediately implanted or cultured further and then implanted. In the latter case, the cells proliferate and secrete new ECM and factors necessary for tissue growth, in vitro, and the biomaterial/tissue construct is then implanted as a graft. Once implanted, the scaffold is also populated by cells from surrounding host tissue. Ideally, for bone regeneration, secretion of a calcified ECM by osteoblasts and subsequent bone growth occur concurrently with scaffold degradation. In the long term, a functional ECM and tissue are regenerated, and are devoid of any residual synthetic scaffold.

Bone regeneration can be achieved by culturing cells capable of expressing the osteoblast phenotype onto synthetic or natural materials that mimic aspects of natural ECMs. Bioceramics that satisfy the design requirements listed above, include bioactive glasses and glass ceramics (Ducheyne et al., 1994; El-Ghannam et al., 1997; Radin et al., 2005; Reilly et al., 2007), HA, TCP, and coral (Ohgushi et al., 1990; Krebsbach et al., 1997, 1998; Yoshikawa et al., 1996; Redey et al., 2000; Kruyt et al., 2004; Holtorf et al., 2005), HA and HA/TCP + collagen (Kuznetsov et al., 1997; Krebsbach et al., 1997, 1998), and polymer/apatite composites (Murphy et al., 2000a; Shin et al., 2007; Segvich et al., 2008a; Hong et al., 2008; Attawia et al., 1995; Thomson et al., 1998). An important consideration is that varying the biomaterial, even subtly, can lead to a significant variation in biological effect in vitro (e.g., osteoblast or progenitor cell attachment and proliferation, collagen and noncollagenous protein synthesis, RNA transcription) (Kohn et al., 2005; Leonova et al., 2006; Puleo et al., 1991; Ducheyne et al., 1994; El-Ghannam et al., 1997; Thomson et al., 1998; Zreiqat et al., 1999; Chou et al., 2005). The nature of the scaffold can also significantly affect in vivo response (e.g., progenitor cell differentiation to osteoblasts, amount and rate of bone formation, intensity or duration of any transient or sustained inflammatory response) (Kohn et al., 2005; Ohgushi et al., 1990; Kuznetsov et al., 1997; Krebsbach et al., 1997, 1998; James et al., 1999; Hartman et al., 2005).

15.4.1 Biomimetic Ceramics

Through millions of years of evolution, the skeleton has evolved into a near-optimally designed system that performs the functions of load bearing, organ protection, and chemical balance efficiently and with a minimum expenditure of energy. Traditional engineering approaches might have accomplished these design goals by using materials with greater mass. However, nature designed the skeleton to be relatively lightweight, because of the elegant design approaches used. First is the ability to adapt to environmental cues, that is, physiological systems are "smart." Second, tissues are hierarchical composites consisting of elegant interdigitations of organic and inorganic constituents that are synthesized via solution chemistry under benign conditions. Third, nature has optimized the orientation of the constituents and developed functionally graded materials, that is, the organic and inorganic phases are heterogeneously distributed to accommodate variations in anatomic demands.

Biomimetic materials, or man-made materials that attempt to mimic biology by recapitulating some of nature's design rules, are hypothesized to lead to a superior biological response. Compared to synthetic materials, natural biominerals reflect a remarkable level of control in their composition, size, shape, and organization at all levels of hierarchy (Weiner, 1986; Lowenstein and Weiner, 1989). A biomimetic mineral surface could therefore promote preferential absorption of biological molecules that regulate cell function, serving to promote events leading to cell-mediated biomineralization. The rationale for using biomimetic mineralization as a material design strategy is based on the mechanisms of biomineralization (Weiner, 1986; Lowenstein and Weiner, 1989; Mann et al., 1988; Mann and Ozin, 1996) and bioactive material function (Sec. 15.3). Bioactive ceramics bond to bone through a layer of bonelike apatite, which forms on the surfaces of these materials in vivo, and is characterized by a carbonate-containing apatite with small crystallites and defective structure (Ducheyne, 1987; Nakamura et al., 1985; Combes and Rey, 2002; Kokubo and Takadama, 2006). This type of apatite is not observed at the interface between nonbioactive materials and bone and it has been suggested, but not universally agreed upon, that nonbioactive materials do not exhibit surface-dependent cell differentiation (Ohgushi and Caplan, 1999). It is therefore hypothesized that a requirement for a biomaterial to bond to bone is the formation of a biologically active bonelike apatite layer (Kohn and Ducheyne, 1992; Ducheyne, 1987; Nakamura et al., 1985; Combes and Rey, 2002; Kokubo and Takadama, 2006).

A bonelike apatite layer can be formed in vitro at STP conditions (Murphy et al., 2000a; Shin et al., 2007; Abe et al., 1990; Li et al., 1992; Bunker et al., 1994; Campbell et al., 1996; Tanahashi et al., 1995; Yamamoto et al., 1997; Wu et al., 1997; Wen et al., 1997), providing a way to control the in vivo response to a biomaterial. The basis for synthesizing bonelike mineral in a biomimetic fashion lies in the observation that in nature, organisms use macromolecules to control mineral nucleation and growth (Weiner, 1986; Bunker et al., 1994). Macromolecules usually contain functional groups that are negatively charged at the crystallization pH (Weiner, 1986), enabling them to chelate ions present in the surrounding media which stimulate crystal nucleation (Bunker et al., 1994). The key requirement is to chemically modify a substrate to induce heterogeneous nucleation of mineral from a solution (Bunker et al., 1994). Biomimetic processes are guided by the pH and ionic concentration of the microenvironment, and conditions conducive to heterogeneous nucleation will support epitaxial growth of mineral (Fig. 15.7). To drive heterogeneous precipitation, the net energy between a nucleated precursor and the substrate must be less than the net energy of the nucleated precursor within the ionic solution (Bunker et al., 1994).

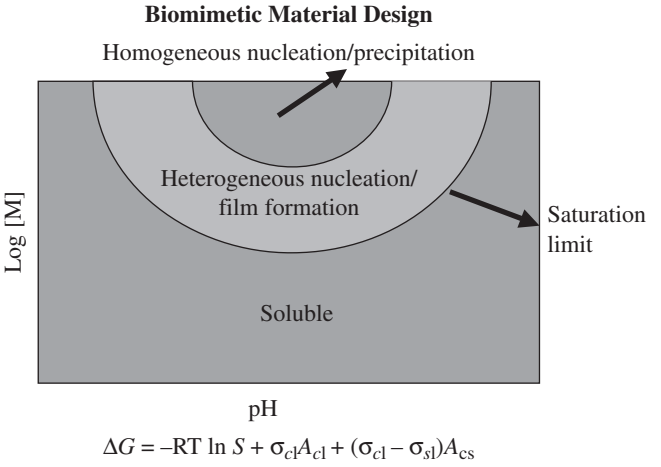

FIGURE 15.7 Schematic of a design space for biomimetic mineralization of materials. Variations in ionic concentration and pH modulate mineral nucleation. Heterogenous nucleation of mineral onto a substrate is the thermodynamically driven design goal. The free energy for crystal nucleation ΔG is a function of the degree of solution supersaturation S, temperature T, crystal interfacial energy σ, crystal surface area A. Subscripts c, s, and l denote interfaces involving the crystal, solid substrate and liquid, respectively.

Surface functionalization may be achieved via grafting, self-assembled monolayers, irradiation, alkaline treatment, or simple hydrolysis (Murphy et al., 2000a; Shin et al., 2007; Segvich et al., 2008a; Tanahashi et al., 1995; Yamamoto et al., 1997; Wu et al., 1997; Hanawa et al., 1998). This biomimetic strategy has been used with metals to accelerate osseointegration (Kohn, 1998; Abe et al., 1990; Campbell et al., 1996; Wen et al., 1997; Hanawa et al., 1998) and, more recently, with glasses, ceramics, and polymers (Murphy et al., 2000a; Shin et al., 2007; Segvich et al., 2008a; Hong et al., 2008; Tanahashi et al., 1995; Yamamoto et al., 1997; Wu et al., 1997; Kamei et al., 1997; Du et al., 1999; Taguchi et al., 1999; Chou et al., 2005).

As an example of this biomimetic strategy, porous polyester scaffolds incubated in a simulated body fluid (SBF, a supersaturated salt solution with a composition and ionic concentrations approximating those of plasma), exhibit coordinated surface functionalization, nucleation and growth of a continuous bonelike apatite layer on the polymer surfaces and within the pores (Fig. 15.8) after relatively short incubation times (Murphy et al., 2000a; Shin et al., 2007; Segvich et al., 2008a). FTIR

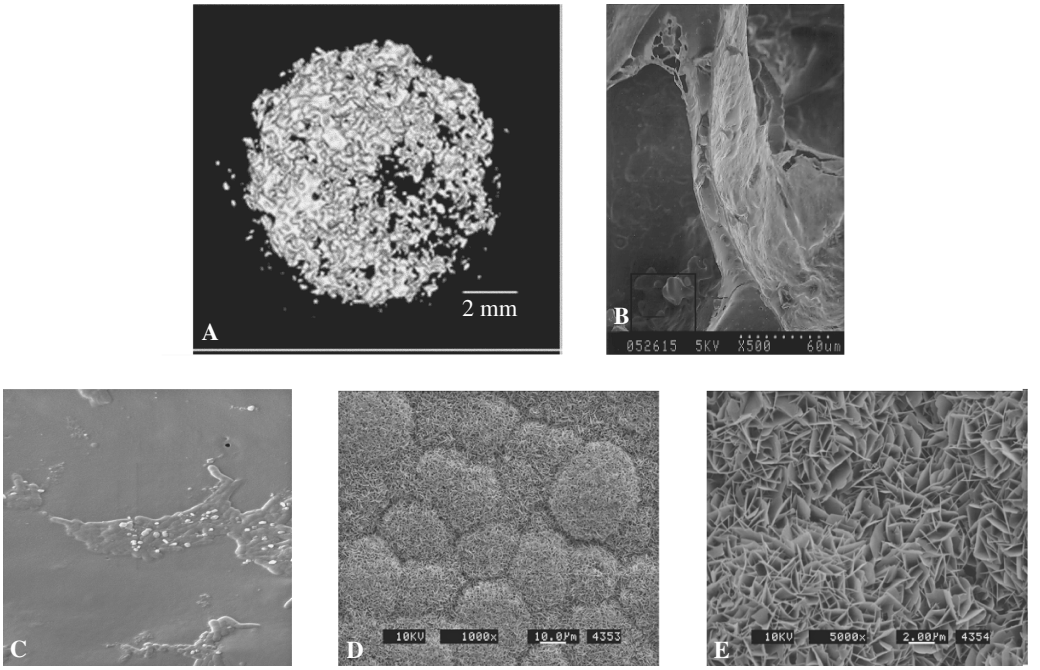

FIGURE 15.8 Images of 85:15 polylactide/glycolide scaffolds incubated in a simulated body fluid (SBF). (*a*) Microcomputed tomography image of whole scaffold showing mineralization through the thickness of the scaffold; (*b*) Localized SEM image of a scaffold cross-section, showing mineralization of a pore wall; (*c*) SEM image of mineral nucleation on hydrolyzed PLGA; (*d*) SEM image of continuous mineral grown on the PLGA—a conglomerated granular structure with needle-shaped precipitates is visible; (*e*) higher magnification SEM image of elongated platelike hexagonal crystals extending out of the plane of the granular structure. [*(a), From Segvich et al. (2008a), with permission; (b), from Murphy et al., (2000a), with permission; (d),(e), from Hong et al. 2008, with permission.*]

analyses confirm the nature of the bonelike mineral, and ability to control mineral composition via controlling the ionic activity product (IP) of the SBF (Fig. 15.9). As IP increases, more mineral grows on the scaffold pore surfaces, but the apatite is less crystalline and the Ca/P molar ratio decreases. Since mineral composition and structure affect cell function, the IP of the mineralization solution is an important modulator of material properties, potentially leading to enhanced control of cell function. Mineralization of the polymer substrate also results in a fivefold increase in compressive modulus, without a significant reduction in scaffold porosity (Murphy et al., 2000a). The increase in mechanical properties with the addition of only a thin bonelike mineral is important in light of the competing design requirements of transport and mechanics, which frequently may only be balanced by choosing an intermediate porosity.

The self-assembly of mineral within the pores of a polymer scaffold enhances cell adhesion, proliferation, and osteogenic differentiation, as well as modulates cytoskeletal organization and cell motility in vitro (Kohn et al., 2005; Leonova et al., 2006). When progenitor cells are transplanted on these materials, a larger and more spatially uniform volume of bone is regenerated, compared to unmineralized templates (Kohn et al., 2005; Rossello, 2007). An additional benefit of the biomimetic processing conditions (e.g., room temperature, atmospheric pressure) is that incorporation of growth factors is achievable, without concern for denaturing, thus enabling a dual conductive/inductive approach (Fig. 15.10) (Murphy et al., 2000b; Luong et al., 2006; Segvich et al., 2008a). Therefore, biomineralized materials can serve as a platform for conductive, inductive, and cell transplantation approaches to regeneration, and fulfill the majority of the design requirements outlined above.

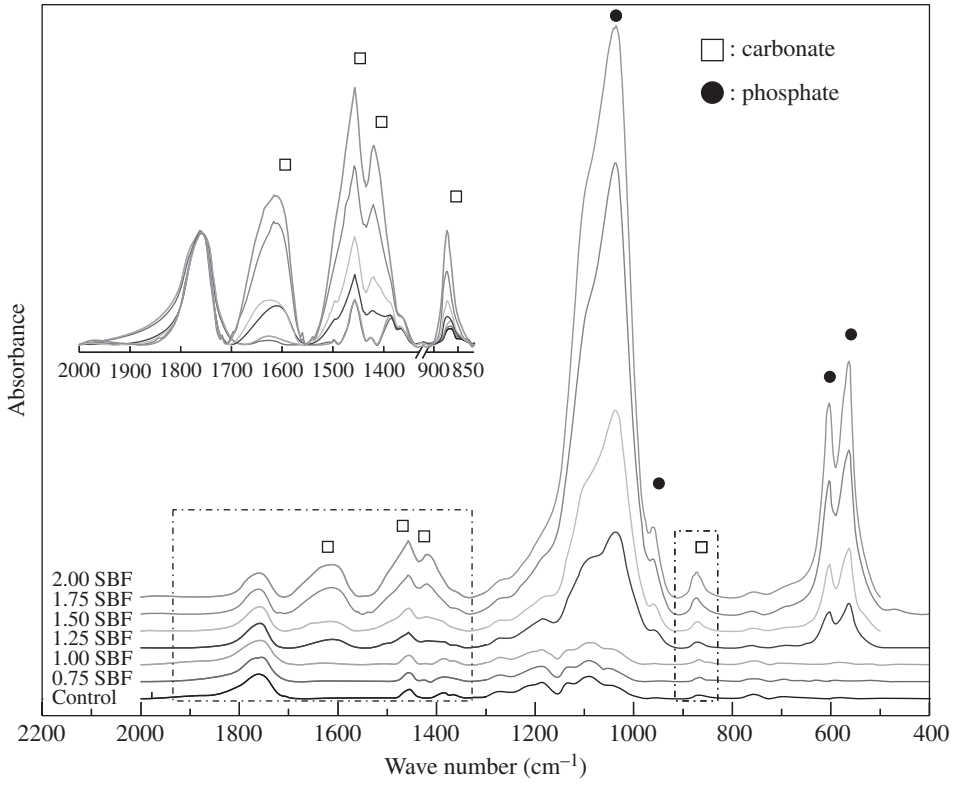

FIGURE 15.9 FTIR spectra of the mineralized pore surfaces of 85:15 PLGA scaffolds incubated in simulated body fluids (SBF) of varying ionic activity products (IP) for 16 days. Inset = bands within the boxes stacked and enlarged to better show changes in CO_3^{2-}. Band intensities of phosphate and carbonate increased with increasing IP. [*From Shin et al. (2007), with permission.*]

15.4.2 Inorganic/Organic Hybrid Biomimetics

Advancements in understanding biomineralization have also resulted in the synthesis of mineral-organic hybrids, consisting of bonelike apatites combined with inductive factors, to control cell proliferation, differentiation, and bone formation (Murphy et al., 2000b; Luong et al., 2006; Segvich et al., 2008a; Liu et al., 2001). The method of combining inorganic mineral with organic factors can influence the resultant release profile, and therefore, influence the biological response of cells. The most basic method of incorporating proteins into ceramics is adsorption, where the factor is loosely bound to the ceramic surface by submersion or pipetting. A second way of incorporating protein with apatite is to create microcarriers that allow HA crystals to form in the presence of protein or allow protein to adsorb to the HA (Ijntema et al., 1994; Barroug and Glimcher, 2002; Matsumoto et al., 2004). A third method of protein incorporation is coprecipitation, in which protein is added to SBF and becomes incorporated into bonelike apatite during calcium-phosphate precipitation. Organic/inorganic hybrids show promise in combining the osteoconductive properties provided by the apatite with the osteoinductive potential provided by growth factors, DNA, and peptides.

Through coprecipitation, BMP-2 has been incorporated into biomimetic coatings deposited on titanium, and biological activity has been retained (Liu et al., 2004). Biomolecules can be incorporated at different stages of calcium-phosphate nucleation and growth (Fig. 15.10) (Luong et al., 2006; Azevedo et al., 2005), enabling spatial localization of the biomolecule through the apatite thickness, and allowing the controlled release of the biomolecule. With spatial localization, there is also the potential for delivery of multiple biomolecules.

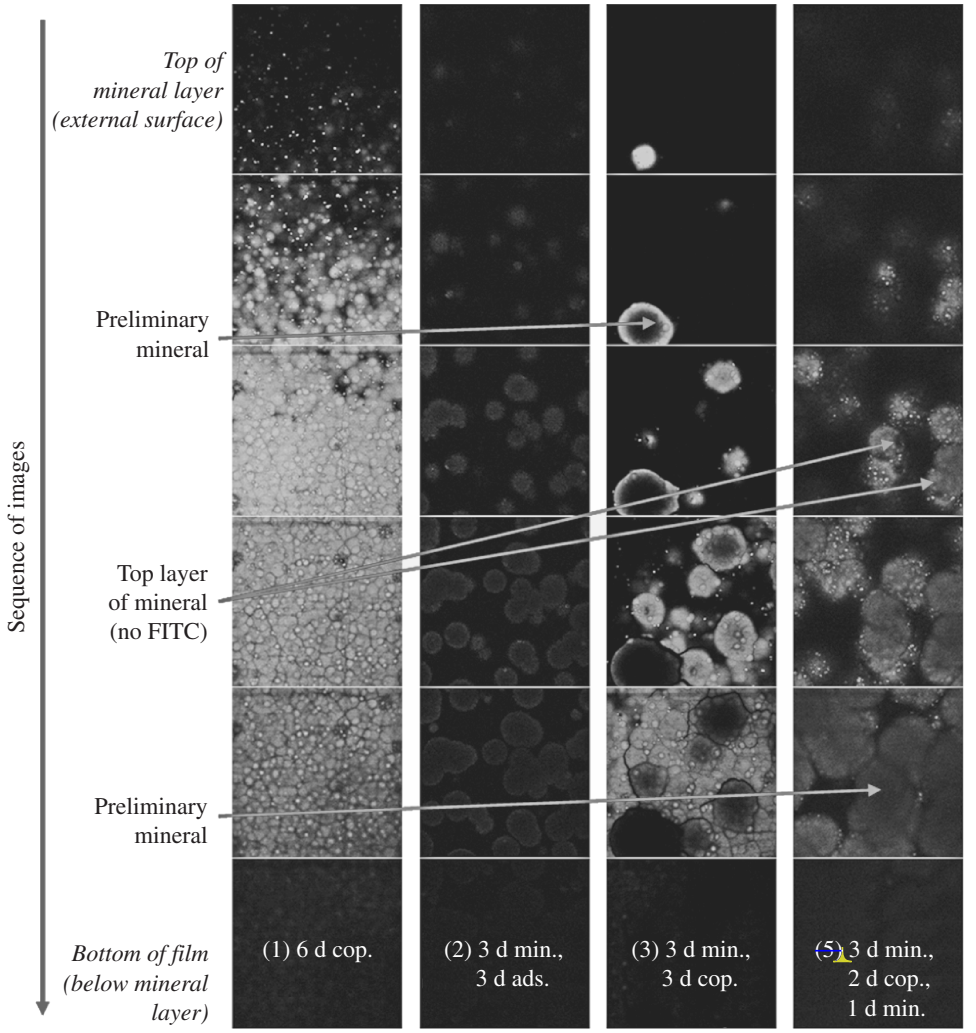

FIGURE 15.10 Images through the thickness of a mineral layer containing FITC-labeled BSA taken using confocal microscopy. Spatial distribution of the protein through the thickness of the mineral is exhibited for the following protein incorporation techniques: (1) 6 days of mineral/BSA coprecipitation; (2) 3 days of mineralization followed by 3 days of protein adsorption; (3) 3 days of mineralization followed by 3 days of mineral/BSA coprecipitation; (5) 3 days of mineralization, followed by 2 days of mineral/BSA coprecipitation, followed by 1 day of mineralization. [*From Luong et al. (2006), with permission from Elsevier.*]

Techniques used to incorporate growth factors into bonelike mineral can also be used to incorporate genes. One of the most common methods of gene delivery is to encapsulate DNA within a Ca-P precipitate (Jordan et al., 1996). This method protects DNA from degradation and encourages cellular uptake, but DNA is released in a burst, which is not always the desired release kinetics. By utilizing coprecipitation to incorporate plasmid DNA into a biomimetic apatite layer, osteoconductivity and osteoinductivity are combined into a single approach that has the ability to transfect host cells. The mineral increases substrate stiffness, which also enhances cellular uptake of plasmid DNA (Kong et al., 2005).

Not only is the method of protein incorporation an integral part of developing an effective delivery system, but the interaction between the biological factor and mineral is also important. Biological factors can alter nucleation, growth, and biomineral properties (e.g., crystal phase, morphology, crystal growth habit, orientation, chirality) (Wen et al., 1999; Azvedo et al., 2005; Liu et al., 2003; Uchida et al., 2004; Combes et al., 1999), changing the osteoconductive capacity of the mineral. When organic constituents are introduced into the mineralizing solution, the dynamics of mineralization change due to changes in pH, interactions between the biological factor and ions in solution, and interactions with the substrate. These dynamics can enhance or inhibit the heterogeneous deposition of mineral onto the substrate.

Following coprecipitation, the release of biological factors and resultant biological responses are influenced by many variables, including the concentration of the factor, the expression of the receptors that are affected by the presence of the factor, the physical characteristics of the delivery substrate and mineral/organic coating, and the site of implantation. Release kinetics can be controlled via diffusion of the biological factor, dissolution/degradation of the carrier and/or osmotic effects. For delivery systems based on coprecipitation of a biological molecule with a biomineral, the dissolution mechanisms of mineral are the most important.

Mineral dissolution is controlled by factors associated with the solution (pH, saturation), bulk solid (solubility, chemical composition), and surface (adsorbed ions, phases). The apatite that is typically formed from a supersaturated ionic solution is carbonated (Murphy et al., 2000a; Shin et al., 2007). The presence of carbonate in an apatite lattice influences crystallinity and solubility (Tang et al., 2003; Ito et al., 1997; Krajewski et al., 2005). The dissolution rate of carbonated HA depends pH, and occurs with the protonation of the carbonate or phosphate group to form either carbonic acid or phosphoric acid (Hankermeyer et al., 2002). Thus, when experimental conditions change, the dissolution properties of mineral and release kinetics of any biomolecules incorporated into the mineral also change.

Apatite that has protein simply adsorbed to its surface undergoes a burst effect, releasing most of the protein within the first 6 hours, whereas less than 1 percent of the protein incorporated within bonelike apatite is released after 5 days (Liu et al., 2001). With coprecipitation, a small burst occurs due to a small amount of protein that is adsorbed to the surface. The resultant sustained release is hypothesized to be due to the incorporation of protein within the apatite matrix, rather than just a superficial association (Liu et al., 2001). The affinity a protein has for apatite influences the dissolution rate of the mineral and, therefore, the release rate. Since protein release is proportional to apatite dissolution, the possibility of temporally controlling the release profile, as well as developing multifactor delivery systems is possible due the ability to spatially localize the protein within the biomimetically nucleated mineral (Luong et al., 2006).

In addition to trying to control cell function via biomolecular incorporation within apatite, another strategy is to present biomolecules on a biomimetic surface. While the objective of coprecipitation is to control spatial and temporal release of biomolecules, the objective of presenting peptides with conformational specificity on a material surface is to recruit a population of cells that can initiate the early stages of bone regeneration. Proteins, growth factors, and peptides have been ionically or covalently attached to biomaterial surfaces to increase cell adhesion, and ultimately, the amount of bone growth. While specific proteins that enhance cell adhesion have been identified, proteins, in general, are subject to isolation and prone to degradation (Hersel et al., 2003). Proteins can also change conformation or orientation because they possess sections with varying hydrophobicities that address cellular functions other than adhesion. On the other hand, peptides can effectively mimic the same response as a protein while being smaller, cheaper, and less susceptible to degradation. Peptides have a greater potential for controlling initial biological activity, because they can contain specific target amino acid sequences and can permit control of hydrophilic properties through sequence design (Ladner et al., 2004).

Identification of cell recognition sequences has motivated the development of bioactive materials that can recruit a desired cell population to adhere to a material surface via specific integrin-mediated bonding. One peptide sequence that interacts with a variety of cell adhesion receptors, including those on osteoblasts, is the RGD (Arg-Gly-Asp) sequence. Other peptide sequences have been designed to mimic sections of the ECM proteins bone sialoprotein, osteopontin, fibronectin, statherin, elastin, and osteonectin (Fujisawa et al., 1996, 1997; Gilbert et al., 2000; Simionescu et al., 2005). Peptide sequences with preferential affinity to HA and bonelike mineral have been discovered using phage display libraries (Segvich et al., 2008b).

15.5 SUMMARY

In summary, bioceramics have a long clinical history, especially in skeletal reconstruction and regeneration. Bioceramics are classified as relatively inert (a minimal tissue response is elicited and a layer of fibrous tissue forms adjacent to the implant), surface active (partially soluble, resulting in surface ion exchange with the microenvironment and leading to a direct chemical bond with tissue), and bulk bioactive (fully resorbable, with the potential to be completely replaced with de novo tissue). Ceramics are processed via conventional materials science strategies, as well as strategies inspired by nature. The biomimetic approaches discussed in Section 15.4, along with all other strategies to reproduce the design rules of biological systems, do not completely mimic nature. Instead, just selected biological aspects are mimicked. However, if the selected biomimicry is rationally designed into biomaterial, then the biological system will be able to respond in a more controlled, predictable, and efficient manner, providing an exciting new arena for biomaterials research and development.

ACKNOWLEDGEMENTS

Parts of the author's research discussed in this chapter were supported by NIH/NIDCR R01 DE 013380 and R01 DE015411.

REFERENCES

Abe, Y., Kokubo, T., Yamamuro, T., *J. Mater. Sci.: Mater. Med.* **1**:233–238, 1990.

Allen, M., Myer, B., Rushton, N., *J. Biomed. Mater. Res. (Appl. Biomat.)* **58**:319–328, 2001.

Attawia, M. A., Devin, J. E., Laurencin, C. T., *J. Biomed. Mater. Res.* **29**:843–848, 1995.

Azevedo, H. S., Leonor, I. B., Alves, C. M., Reis, R. L., *Mat. Sci. Eng. C.—Bio. S.* **25**:169, 2005.

Barroug, A., Glimcher, M. J., *J. Orthop. Res.* **20**:274, 2002.

Bokros, J. C., *Trans. Biomed. Mater. Res. Symp*. **2**:32–36, 1978.

Bokros, J. C., LaGrange, L. D., Schoen, G. J., In: *Chemistry and Physics of Carbon*, Vol. 9, Walker, P. L., (ed.), New York, Dekker, pp. 103–171, 1972.

Boutin, P., Christel, P., Dorlot, J. M., Meunier, A., de Roquancourt, A., Blanquaert, D., Herman, S., Sedel, L., Witvoet, J., *J. Biomed. Mater. Res.* **22**:1203–1232, 1988.

Bunker, B. C., Rieke, P. C,, Tarasevich, B. J., Campbell, A. A., Fryxell, G. E., Graff, G. L., Song, L., Liu, J., Virden, J. W., McVay, G. L., *Science* **264**:48–55, 1994.

Cales, B., Stefani, Y., In: *Biomedical Engineering Handbook*, Bronzino, J. D., (ed.), Boca Raton, FL, CRC Press, pp. 415–452, 1995.

Campbell, A. A., Fryxell, G. E., Linehan, J. C., Graff, G. L., *J. Biomed. Mater. Res.* **32**:111–118, 1996.

Chai, C. S., Gross, K. A., Ben-Nissan, B., *Biomat* **19**:2291–2296, 1998.

Chou, Y. F., Huang, W., Dunn, J. C. Y., Miller, T. A., Wu, B. M., *Biomat* **26**:285–295, 2005.

Christel, P., Meunier, A., Heller, M., Torre, J. P., Peille, C. N., *J. Biomed. Mater. Res.* **23**:45–61, 1989.

Christel, P., Meunier, A., Leclercq, S., Bouquet, P., Buttazzoni, B., *J. Biomed. Mater. Res.: Appl. Biomat.* **21**(A2):191–218, 1987.

Combes, C., Rey, C., *Biomat* **23**:2817–2823, 2002.

Combes, C., Rey, C., Freche, M., *J. Mater. Sci. Mater. Med.* **10**:153, 1999.

Cook, S. D., Thomas, K. A., Dalton, J. E., Volkman, T. K., Whitecloud, T. S., III, Kay, J. F., *J. Biomed. Mater. Res.* **26**:989–1001, 1992.

Davidson, J. A., *Clin. Orthop.* **294**:361–178, 1993.

de Bruijn, J. D., van Blitterswijk, C. A., Davies, J. E., *J. Biomed. Mater. Res.* **29**: 89–99, 1995.

de Groot, K., (ed.), *Bioceramics of Calcium Phosphate*, Boca Raton, FL, CRC Press, 1983.

de Groot, K., Geesink, R. G. T., Klein, C. P. A. T., Serekian, P., *J. Biomed. Mater. Res.* **21**:1375–1381, 1987.

Derbyshire, B., Fisher, J., Dowson, D., Hardaker, C., Brummitt, K., *Med. Eng. Phys.* **16**:229–236, 1994.

Dorre, E., Dawihl, W., In: *Mechanical Properties of Biomaterials*, Hastings, G. W., Williams, D. F., (eds.), New York, Wiley, pp. 113–127, 1980.

Du, C., Cui, F. Z., Zhu, X. D., de Groot, K., *J. Biomed. Mater. Res.* **44**:407–415, 1999.

Ducheyne, P., *J. Biomed. Mater. Res.* **19**:273–291, 1985.

Ducheyne, P., *J. Biomed. Mater. Res.: Appl. Biomat.* **21**(A2):219–236, 1987.

Ducheyne, P., Hench, L. L., Kagan, A., II, Martens, M., Bursens, A., Mulier, J. C., *J. Biomed. Mater. Res.* **14**:225–237, 1980.

Ducheyne, P., El-Ghannam, A., Shapiro, I., *J. Cell Biochem.* **56**:162–167, 1994.

Ducheyne, P., Radin, S., Heughebaert, M., Heughebaert, J. C., *Biomat.* **11**:244–254, 1990.

Ducheyne, P., Van Raemdonck, W., Heughebaert, J. C., Heughebaert, M., *Biomat.* **7**:97–103, 1986.

El-Ghannam, A., Ducheyne, P., Shapiro, I. M., *J. Biomed. Mater. Res.* **36**:167–180, 1997.

Filiaggi, M. J., Coombs, N. A., Pilliar, R. M., *J. Biomed. Mater. Res.* **25**:1211–1229, 1991.

Filiaggi, M. J., Pilliar, R. M., Yakubovich, R., Shapiro, G., *J. Biomed. Mater. Res. (Appl. Biomat.)* **33**:225–238, 1996.

Fujisawa, R., Mizuno, M., Nodasaka, Y., Kuboki, Y., *Matrix Biol.* **16**:21, 1997.

Fujisawa, R., Wada, Y., Nodasaka, Y., Kuboki, Y., *Biochim. Biophys. Acta* **1292**:53, 1996.

Gao, Y., In: *Biomedical Materials—Drug Delivery, Implants and Tissue Engineering*, Neenan, T ., Marcolongo, M., Valentini, R. F., (eds.), Materials Research Society, Warrendale, PA, pp. 361–366, 1999.

Garcia, F., Arias, J. L., Mayor, B., Pou, J., Rehman, I., Knowles, J., Best, S., Leon, B., Perez-Amor, M., Bonfield, W., *J. Biomed. Mater. Res. (Appl. Biomat.)* **43**:69–76, 1998.

Gilbert, M., Shaw, W. J., Long, J. R., Nelson, K., Drobny, G. P., Giachelli, C. M., Stayton, P. S., *J. Biol. Chem.* **275**:16213, 2000.

Gross, U., Brandes, J., Strunz, V., Bab, I., Sela, J., *J. Biomed. Mater. Res.* **15**:291–305, 1981.

Gross, U., Strunz, V., *J. Biomed. Mater. Res.* **14**:607–618, 1980.

Gross, U., Strunz, V., *J. Biomed. Mater. Res.* **19**:251–271, 1985.

Hanawa, T., Kon, M., Ukai, H., Murakami, K., Miyamoto, Y., Asaoka, K., *J. Biomed. Mater. Res.* **41**:227–236, 1998.

Hankermeyer, C. R., Ohashi, K. L., Delaney, D. C., Ross, J., Constantz, B. R., *Biomaterials* **23**:743, 2002.

Hartman, E. H. M, Vehof, J. W. M., Spauwen, P. H. M., Jansen, J. A., *Biomaterials* **26**:1829–1835, 2005.

Haubold, A. D., Shim, H. S., Bokros, J. C., In: *Biocompatibility of Clinical Implant Materials*, Vol. II, Williams, D. F., (ed.), Boca Raton, FL, CRC Press, pp. 3–42, 1981.

Heimke, G., Jentschura, G., Werner, E., *J. Biomed. Mater. Res.* **12**:57–65, 1978.

Hench, L. L., Best, S., In: *Biomaterials Science: An Introduction to Materials in Medicine,* 2nd ed*,* Ratner, B. D., Hoffman, A. S., Schoen, F. J., Lemons, J. E., (eds.), San Diego, Elsevier Academic Press, pp. 153–169, 2004.

Hench, L. L, Clark, A. E., In: *Biocompatibility of Orthopaedic Implants*, Vol. II, Williams, D. F., (ed.), Boca Raton, FL, CRC Press, pp. 129–170, 1982.

Hench, L. L., Ethridge, E. C., *Biomaterials An Interfacial Approach*, New York, Academic Press, 1982.

Hench, L. L., Splinter, R. J., Allen, W. C., Greenlee, T. K., Jr., *J. Biomed. Mater. Res. Symp.* **2**:117–141, 1972.

Hersel, U., Dahmen, C., Kessler, H., *Biomaterials* **24**:4385, 2003.

Holtorf, H. L., Sheffield, T. L., Ambrose, C. G., Jansen, J. A., Mikos, A. G., *Ann. Biomed. Eng.* **33**:1238–1248, 2005.

Hong, S. I., Lee, K. H., Outslay, M. E., Kohn, D. H., *J. Mater. Res.* **23**:478–485, 2008.

Hulbert, S. F., Young, F. A., Mathews, R. S., Klawitter, J. J., Talbert, C. D., Stelling, F. H., *J. Biomed. Mater. Res.* **4**:433–456, 1970.

Huttner, W., Huttinger, K. J., In: *The Cementless Fixation of Hip Endoprostheses*, Morscher, E., (ed.), Berlin, Springer-Verlag, pp. 81–94, 1984.

Ijntema, K., Heuvelsland, W. J. M., Dirix, C., Sam, A. P., *Int. J. Pharm.* **112**:215, 1994.

Ioku, K., Yoshimura, M., Somiya, S., *Biomaterials* **11**:57–61, 1990.

Ito, A., Maekawa, K., Tsutsumi, S., Ikazaki, F., Tateishi, T., *J. Biomed. Mater. Res.* **36**:522, 1997.

James, K., Levene, H., Parson, J. R., Kohn, J., *Biomaterials* **20**:2203–2212, 1999.

Jordan, M., Schallhorn, A., Wurm, F. M., *Nucleic. Acids Res.* **24**:596, 1996.

Kamei, S., Tomita, N., Tamai, S., Kato, K., Ikada, Y., *J. Biomed. Mater. Res.* **37**:384–393, 1997.

Kitsugi, T., Yamamuro, T., Nakamura, T., Higashi, S., Kakutani, Y., Hyakuna, K., Ito, S., Kokubo, T., Takagi, M., Shibuya, T., *J. Biomed. Mater. Res.* **20**:1295–1307, 1986.

Knowles, J. C., Bonfield, W., *J. Biomed. Mater. Res.* **27**:1591–1598, 1993.

Ko, C. C., Kohn, D. H., Hollister, S. J., *J. Mater. Sci.: Mater. Med.* **7**:109–117, 1995.

Koch, B., Wolke, J. G. C., de Groot, K., *J. Biomed. Mater. Res.* **24**:655–667, 1990.

Koeneman, J., Lemons, J., Ducheyne, P., Lacefield, W., Magee, F., Calahan, T., Kay, J., *J. Appl. Biomat.* **1**:79–90, 1990.

Kohn, D. H., *Curr. Opin. Solid State Mater. Sci.* **3**:309–316, 1998.

Kohn, D. H., Ducheyne, P., "Materials for Bone, Joint and Cartilage Replacement," In: *Medical and Dental Materials*, Williams, D. F. (ed.), VCH Verlagsgesellschaft, FRG, pp. 29–109, 1992.

Kohn, D. H., Shin, K., Hong, S. I., Jayasuriya, A. C., Leonova, E. V., Rossello, R. A., Krebsbach, P. H., In: *Proc. 8th Int. Conf. on the Chemistry and Biology of Mineralized Tissues*, Landis, W. J., Sodek, J., (eds.), University of Toronto Press, pp. 216–219, 2005.

Koistinen, A., Santavirta, S. S., Kroger, H., Lappalainen, R., *Biomaterials* **26**:5687–5694, 2005.

Kokubo, T., Ito, S., Huang, Z. T., Hayashi, T., Sakka, S., Kitsugi, T., Yamamuro, T., *J. Biomed. Mater. Res.* **24**:331–343, 1990a.

Kokubo, T., Kushitani, H., Sakka, S., Kitsugi, T., Yamamuro, T., *J. Biomed. Mater Res.* **24**:721–734, 1990b.

Kokubo, T., Takadama, H., *Biomaterials* **27**:2907–2915, 2006.

Kong, H. J., Liu, J. D., Riddle, K., Matsumoto, T., Leach, K., Mooney, D. J., *Nat. Mater.* **4**:460, 2005.

Krajewski, A., Mazzocchi, M., Buldini, P. L., Ravaglioli, A., Tinti, A., Taddei, P., Fagnano, C., *J. Mol. Struct.* **744**:221, 2005.

Krebsbach, P. H., Kuznetsov, S. A., Satomura, K., Emmons, R. V. B., Rowe, D. W., Gehron-Robey, P., *Transplantation* **63**:1059–1069, 1997.

Krebsbach, P. H., Mankani, M. H., Satomura, K., Kuznetsov, S. A., Gehron-Robey, P., *Transplantation* **66**:1272–1278, 1998.

Kruyt, M. C., Dhert, W. J. A., Yuan, H., Wilson, C. E., van Blitterswijk, C. A., Verbout, A. J., de Bruijn, J. D., *J. Orthop. Res.* **22**:544–551, 2004.

Kumar, P., Oka, M., Ikeuchi, K., Shimizu, K., Yamamuro, T., Okumura, H., Kotoura, Y., *J. Biomed. Mater. Res.* **25**:813–828, 1991.

Kuznetsov, S. A., Krebsbach, P. H., Satomura, K., Kerr, J., Riminucci, M., Benayahu, D., Gehron-Robey, P., *J. Bone Min. Res.* **12**:1335–1347, 1997.

Ladner, R. C., Sato, A. K., Gorzelany, J., de Souza, M., *Drug Discov. Today* **9**:525, 2004.

Laurencin, C. T., El-Amin, S. F., Ibim, S. E., Willoughby, D. A., Attawia, M., Allcock, H. R., Ambrosio, A. A., *J. Biomed. Mater. Res.* **30**:133–138, 1996.

Leonova, E. V., Pennington, K. E., Krebsbach, P. H., Kohn, D. H., *J. Biomed. Mater. Res. Part A* **79A**:263–270, 2006.

Li, J., Fartash, B., Hermansson, L., *Biomaterials* **16**:417–422, 1995.

Li, P., Ohtsuki, C., Kokubo, T., Nakanishi, K., Soga, N., Nakamura, T., Yamamuro, T., *J. Am. Ceram. Soc.* **75**:2094–2097, 1992.

Liu, Y., Hunziker, E. B., Randall, N. X., de Groot, K., Layrolle, P., *Biomaterials* **24**:65, 2003.

Liu, Y. L., Hunziker, E. B., Layrolle, P., de Bruijn, J. D., de Groot, K., *Tissue Eng* **10**:101–108, 2004.

Liu, Y. L., Layrolle, P., de Bruijn, J., van Blitterswijk, C., de Groot, K., *J. Biomed. Mater. Res.* **57**:327, 2001.

Lowenstein, H. A., Weiner, S., *On Biomineralization*, Oxford University Press, Oxford, 1989.

Luong, L. N., Hong, S. I., Patel, R. J., Outslay, M. E., Kohn, D. H., *Biomaterials* **27**:1175–1186, 2006.

Lusty, P. J., Watson, A., Tuke, M. A., Walter, W. L., Walter, W. K., Zicat, B., *J. Bone Joint Surg.* **89B**:1158–1164, 2007.

Mann, K. A., Edidin, A. A., Kinoshita, R. K., Manley, M. T., *J. Appl. Biomat.* **5**:285–291, 1994.

Mann, S., Heywood, B. R., Rajam, S., Birchall, J. D., *Nature* **334**:692–695, 1988.

Mann, S., Ozin, G. A., *Nature* **382**:313–318, 1996.

Matsumoto, T., Okazaki, M., Inoue, M., Yamaguchi, S., Kusunose, T., Toyonaga, T., Hamada, Y., Takahashi, J., *Biomaterials* **25**:3807, 2004.

Miller, R. A., Smialek, R. G., Garlick, In: *Advances in Ceramics,* Vol. 3, *Science and Technology of Zirconia*, Westerville, OH, American Ceramic Society, p. 241, 1981.

Murphy, W. L., Kohn, D. H., Mooney, D.J., *J. Biomed. Mater. Res.* **50**:50–58, 2000a.

Murphy, W. L., Peters, M. C., Kohn, D. H., Mooney, D. J., *Biomaterials* **21**:2521–2527, 2000b.

Nakamura, T., Yamamuro, T., Higashi, S., Kokubo, T., Ito, S., *J. Biomed. Mater. Res.* **19**:685–698, 1985.

Nizard, R., Pourreyron, D., Raould, A., Hannouche, D., Sedel, L., *Clin. Orthop. Rel. Res.* **466**:317–323, 2008.

Ohgushi, H., Caplan, A. I., *J. Biomed. Mater. Res. (Appl. Biomat.)* **48**:913–927, 1999.

Ohgushi, H., Okumura, M., Tamai, S., Shors, E. C., Caplan, A. I., *J. Biomed. Mater. Res.* **24**:1563–1570, 1990.

Ong, J. L., Harris, L. A., Lucas, L. C., Lacefield, W. R., Rigney, E. D., *J. Am. Ceram. Soc.* **74**:2301–2304, 1991.

Oonishi, H., Noda, T., Ito, S., Kohda, A., Ishimaru, H., Yamamoto, M., Tsuji, E., *J. Appl. Biomat.* **5**:23–37, 1994.

Posner, A. S., *Clin. Orthop.* **200**:87–99, 1985a.

Posner, A. S., *J. Biomed. Mater. Res.* **19**:241–250, 1985b.

Puleo, D. A., Holleran, L. A., Doremus, R. H., Bizios, R., *J. Biomed. Mater. Res.* **25**:711–723, 1991.

Redey, S. A., Nardin, M., Bernache-Assolant, D., Rey, C., Delannoy, P., Sedel, L., Marie, P. J., *J. Biomed. Mater. Res.* **50**:353–364, 2000.

Radin, S., Reilly, G., Bhargave, G., Leboy, P. S., Ducheyne, P., *J. Biomed. Mater. Res.* **73A**:21–29, 2005.

Reikeras, O., Johansson, C. B., Sundfeldt, M., *J. Long Term Effects of Med. Impl.* **14**:443–454, 2004.

Reilly, G. C., Radin, S., Chen, A. T., Dycheyne, P., *Biomaterials* **28**:4091–4097, 2007.

Ritter, J. E., Jr., Greenspan, D. C., Palmer, R. A., Hench, L. L., *J. Biomed. Mater. Res.* **13**:251–263, 1979.

Rossello, R. A., Ph.D. Dissertation, University of Michigan, 2007.

Segvich, S. J., Biswas, S., Becker, U., Kohn, D. H., *Cells Tissues Organs,* ~~in press, 2008b.~~

Segvich, S. J., Luong, L. N., Kohn, D. H., "Biomimetic Approaches to Synthesize Mineral and Mineral/Organic Biomaterials," In: *Biomaterials and Biomedical Engineering*, Ahmed, W., Ali, N., Öchsner, A., (eds.), Trans Tech Publications, Ltd, UK, 2008c.

Segvich, S. J., Smith, H. C., Luong, L. N., Kohn, D. H., *J. Biomed. Mater. Res., Part B,* **84B**:340–349, 2008a.

Semlitsch, M., Lehmann, M., Weter, H., Dorre, E., Willert, H. G., *J. Biomed. Mater. Res.* **11**:537, 1977.

Shi, X., Hudson, J. L., Spicer, P. P., Tour, J. M., Krishnamoorti, R., Mikos, A. G., *Biomacromol* **7**:2237–2242, 2006.

Shin, K., Jayasuriya, A. C., Kohn, D. H., *J. Biomed. Mater. Res. Part A,* **83A**:1076–1086, 2007.

Simionescu, A., Philips, K., Vyavahare, N., *Biochem Biophys Res Commun,* **334**:524–532, 2005.

Soltesz, U., Richter, H., In: *Metal and Ceramic Biomaterials Volume II Strength and Surface*, Ducheyne, P., Hastings, G. W., (eds.), Boca Raton, FL, CRC Press pp. 23–61, 1984.

Taguchi, T., Shiraogawa, M., Kishida, A., Arashi, M., *J. Biomater. Sci. Polymer Edn.* **10**:19–31, 1999.

Tanahashi, M., Yao, T., Kokubo, T., Minoda, T., Miyamoto, T., Nakamura, T., Yamamuro, T., *J. Biomed. Mater. Res.* **29**:349–357, 1995.

Tang, R. K., Henneman, Z. J., Nancollas, G. H., *J. Cryst. Growth* **249**:614, 2003.

Thomson, R. C., Yaszemski, M. J., Powers, J. M., Mikos, A. G., *Biomaterials* **19**:1935–1943, 1998.

Tohma, Y., Tanaka, Y., Ohgushi, H., Kawate, K., Taniguchi, A., Hayashi, K., Isomoto, S., Takakura, Y., *J. Orthop. Res.* **24**:595–603, 2006.

Uchida, M., Oyane, A., Kim, H. M., Kokubo, T., Ito, A., *Adv, Mater.* **16**:1071, 2004.

Van Raemdonck, W., Ducheyne, P., De Meester, P., In: *Metal and Ceramic Biomaterials Volume II Strength and Surface*, Ducheyne, P., Hastings, G. W., (eds.), Boca Raton, FL, CRC Press, pp. 143–166, 1984.

Walter, A., Lang, W., In: *Biomedical Materials*—Mater. Res. Soc. Symp. Proc. Vol. 55, Williams, J. M., Nichols, M. F., Zingg, W., (eds.), Pittsburgh, PA, Materials Research Society, pp. 181–190, 1986.

Webster, T. J., Ergun, C., Doremus, R. H., Siegel, R. W., Bizios, R., *J. Biomed. Mater. Res.* **51**:475–483, 2000.

Weiner, S., *CRC Crit Rev Biochem.* **20**:365–408, 1986.

Wen, H. B., de Wijn, J. R., Cui, F. Z., de Groot, K., *J. Biomed. Mater. Res.* **35**:93–99, 1997.

Wen, H. B., de Wijn, J. R., van Blitterswijk, C. A., de Groot, K., *J. Biomed. Mater. Res.* **46**:245, 1999.

Wolke, J. G. C., van Dijk, K., Schaeken, H. G., de Groot, K., Jansen, J. A., *J. Biomed. Mater. Res.* **28**:1477–1484, 1994.

Wu, W., Zhuang, H., Nancollas, G. H., *J. Biomed. Mater. Res.* **35**:93–99, 1997.

Yamamoto, M., Kato, K., Ikada, Y., *J. Biomed. Mater. Res.* **37**:29–36, 1997.

Yaszemski, M. J., Payne, R. G., Hayes, W. C., Langer, R. S., Mikos, A. G., *Biomaterials* **17**:175–185, 1996.

Yoshikawa, T., Ohgushi, H., Tamai, S., *J. Biomed. Mater. Res.* **32**:481–492, 1996.

Zanello, L. P., Zhao, B., Hu, H., Haddon, R. C., *Nano Letters* **6**:562–567, 2006.

Zreiqat, H., Evans, P., Howlett, C. R., *J. Biomed. Mater. Res.* **44**:389–396, 1999.